MATHEMATICAL MODELING AND SIMULATION OF ADSORPTION PROCESS IN A FIXED BED OF MOLECULARLY IMPRINTED POLYMERIC PEARLS

Ştefan-Ovidiu DIMA[1], Tănase DOBRE[2]

In this paper it is developed and applied a mathematical model for the study of the adsorption (and later desorption) processes in a fixed bed of molecularly imprinted polymeric pearls with affinity towards diosgenin. Molecularly imprinted polymers (MIPs) are polymeric materials with high affinity for the molecule they were imprinted with, property that makes them desirable for applications that require high purity compounds or low detection limits in sensing applications. Using the developed model, it was studied the influence of different working parameters like the solvent/ solution flow rate, the height of pearls' bed, and the initial concentrations of adsorbates.

Keywords: mathematical modeling, simulation, adsorption, molecular imprinting

1. Introduction

Molecularly imprinted polymers (MIPs) are a type of extremely selective materials that can be designed according to the desire of the end-user, being known also as artificial antibodies [1-5]. That is the reason why their application area is extremely vast and in continuous expansion, ranging from pharmaceutical industry, biomedical science, engineering, sensors and biosensors, environment protection, analytical applications and others [6-11].

In brief, a MIP is a polymer which is designed to be selective for a target molecule called template by a reverse lock & key mechanism, meaning the lock is build around the key aiming to include as much as possible from the key pattern in order to increase the lock's affinity [12-15]. For reaching a high affinity for the desired target molecule, four main building mechanisms were applied during time: the covalent approach, the non-covalent approach, the alternative method and the ion imprinting method. Each mechanism has as individual characteristic the type of bonds that are being created during the imprinting process, the present

[1] Postdoc., Dept. of Chemical and biochemical Engineering, Faculty of Applied Chemistry and Materials Science, University POLITEHNICA of Bucharest, and Dept. of Bioresources, INCDCP-ICECHIM Bucharest, Romania, e-mail: dr.ovidiu.dima@gmail.com

[2] Prof., Dept. of Chemical and biochemical Engineering, Faculty of Applied Chemistry and Materials Science, University POLITEHNICA of Bucharest, Romania, e-mail: tghdobre@gmail.com

paper dealing with the alternative imprinting mechanism by which the molecularly imprinted pearls were obtained and which will be briefly described in section 2 – Experiment preparation.

In the light of these aspects, the knowledge of understanding and predicting, using mathematical modeling, the pattern by which a molecule would be adsorbed and then desorbed in/from a MIP or a MIP-kind material becomes more than necessary. As semi-empirical method, the mathematical modeling and simulation based on experimental data represents a useful method for understanding and predicting reaction mechanisms and process evolution [16-18]. The mathematical study of the adsorption phenomenon in MIPs started with the application of the well known adsorption models of Langmuir and Freundlich, followed by Scatchard plot and later by the adsorption models of Jovanovic, Temkin, Halsey, Dubinin-Radushkevic, etc., while today hybrid models containing bi-, tri-, or multi-models of adsorption isotherms are applied [19-23].

Starting from the well known adsorption-desorption laws that describe the mass transfer and implementing the concept by which a designed MIP will specifically adsorb the target molecule, it was designed as instrument the present mathematical model, which represents also the aim of the paper.

2. Experiment preparation for fixed bed adsorption experiments

As mentioned in the Introduction, the molecular imprinting mechanism that will be studied by mathematical modeling is the alternative approach. The concept of alternative molecular imprinting was introduced in 1994 [24] and was further developed [25,26], and represents an easy way to introduce molecular recognition sites into polymeric materials starting from polymers and not from monomers. This method can be found also under the names of phase inversion or coagulation, the template-matrix system being stabilized by the curdling of the template-matrix solution in a non-solvent (wet phase inversion) or in a gas (dry phase inversion). Compared to the cross-linking methods that lead to rigid, insoluble MIPs, the alternative molecular imprinting has some advantages: the MIPs prepared by this technique are more easily synthesized and more flexible, can be cast as membranes or pearls, can be cast on the surface of a glassy carbon electrode (GCE) to obtain sensors, and can be recycled by dissolving in a suitable solvent.

Using the alternative molecular imprinting method, diosgenin-selective pearls were previously obtained in three copolymer matrices having three different acrylonitrile:acrylic acid monomer ratios (90:10, 80:20, and 70:30). For the fixed-bed adsorption-desorption experiments, the pearls with the highest imprinting factor, MIP-AN:AA-80:20, and the corresponding non-imprinted pearls (NIP-AN:AA-80:20) will be used.

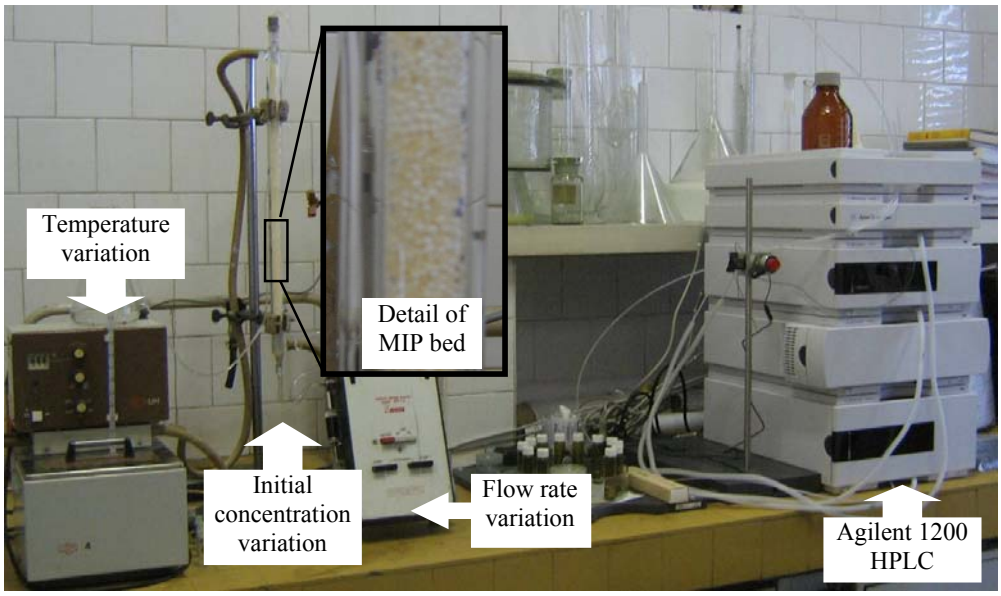

Fig. 1. The laboratory installation for studying thee adsorption-desorption processes in a fixed bed of MIP pearls.

The laboratory installation that was assembled for the mass transfer experiments is presented in *Fig. 1* and consists in a glass column packed with polymer pearls and having a heating jacket, a water thermostat with recirculation pump, a microdose pump for feeding the column, and as analytic equipment an Agilent 1200 HPLC with refractive index detector (RID). The obtained experimental curves (presented in *Fig. 5*) were used to establish the range of some model parameters, for example $Q_L = 6..10 \cdot 10^{-5}$ mol/L, $D_L = 1..2 \cdot 10^{-5}$ cm^2/s, and other parameters mentioned in *table 1*.

3. Theoretical aspects of adsorption-desorption modeling in a fixed bed

Similar to the adsorption processes or ionic exchange on a fixed bed of adsorbents, the adsorption on a fixed bed of MIPs and NIPs is determined by the flow rate of the feeding solution, the bed height, and the MIPs (respectively NIPs) adsorption parameters. The breakthrough curves evidence the adsorption capacity of the MIPs. All the equations used for the breakthrough curves in other fixed bed adsorption processes can be applied for the fixed bed with MIPs [27, 28].

The complexity of the model is dependent on the complexity of the considered sub-models in characterization of the adsorption dynamics. The following considerations will be taken into account:

- the fluid flow through the pearls bed corresponds to the hydrodynamic model **plug flow** with the velocity v perturbed by the axial dispersion D_L;

- the retention kinetics in solid for the target species is determined by the competition between an attachment process and a releasing process.

- the transport processes inside the MIP particle have a negligible rate compared with the attachment rate;

- in solid, the local concentration has the notation c_s, while in the flowing liquid has the notation c, with the subscript A or B for the two competitors.

For a fixed bed of MIP pearls with the height H, the equation of the model and the univocity conditions for the adsorption case with two competitors are:

- the balance equation for specie A in the flowing liquid through the MIP bed:

$$\frac{\partial c_A}{\partial \tau} + v\frac{\partial c_A}{\partial z} = D_L \frac{\partial^2 c_A}{\partial z^2} - v_{RA} \tag{1}$$

- the univocity conditions associated to the concentration field of A species in the flowing liquid:

$$\tau = 0, 0 < \mathrm{z} < \mathrm{H}, \mathrm{c_A} = f_1(z) = 0 \tag{2}$$

$$\tau > 0, \mathrm{z} = 0, \mathrm{c_A} = c_{A0} \tag{3}$$

$$\tau > 0, \mathrm{z} = \mathrm{H}, \mathrm{v}(\mathrm{c_{AH}} - c_{AH}^{+}) = -D_L \frac{dc_A}{dz} \tag{4}$$

- the characteristic equation for the retention of component A inside of MIP, simplified to a first order kinetic:

$$v_{RA} = -\frac{dc_{SA}}{d\tau} = k_{1A}\left((1 - \frac{a_{1A}c_{SA} + b_{1A}c_{SB}}{Q_{LA}}\right)c_A - k_{2A}c_{SA} \tag{5}$$

- the initial condition associated to the kinetic expression of component A retention:

$$\tau = 0, 0 < \mathrm{z} < \mathrm{H}, \mathrm{c_{SA}} = f_2(z) = 0 \tag{6}$$

- the balance equation for specie B in liquid flowing through the MIP fixed bed:

$$\frac{\partial c_B}{\partial \tau} + v\frac{\partial c_B}{\partial z} = D_L \frac{\partial^2 c_B}{\partial z^2} - v_{RB} \tag{7}$$

- the univocity conditions associated to the field of concentration for B specie in liquid flowing through the MIP fixed bed:

$$\tau = 0, 0 \prec \mathrm{z} \prec \mathrm{H}, \mathrm{c_B} = f_2(z) = 0 \tag{8}$$

$$\tau > 0, \mathrm{z} = 0, \mathrm{c_B} = c_{B0} \tag{9}$$

$$\tau > 0, \mathrm{z} = \mathrm{H}, \mathrm{v}(\mathrm{c_{BH}} - c_{BH}^{+}) = -D_L \frac{dc_B}{dz} \tag{10}$$

- the expression characteristic for the retaining of B component inside the MIP:

$$v_{RB} = -\frac{dc_{SB}}{d\tau} = k_{1B}\left((1-\frac{a_{1B}c_{SA}+b_{1B}c_{SB}}{Q_{LB}}\right)c_B - k_{2B}c_{SB} \tag{11}$$

A suitable modification of the univocity and initial conditions, as of model's parameters (v, D_L, a_{1A}, b_{1A}, k_{1A}, k_{2A}, Q_{LA}, a_{1B}, b_{1B}, k_{1B}, k_{2B}, Q_{LB}) transforms the model, from an adsorption model into an elution model for the species on the MIP particles bed.

The elution model results from the adsorption model by excluding the kinetic adsorption terms and making adequate the univocity conditions. If the *v* and D_L parameters are easy to measure, the number of 10 parameters remains too large to be estimated from the dynamic measurements. In consequence, for identification of some of the parameters are needed other experimental measurements, like the ones at equilibrium.

The *table 1* presents the organizing of the numerical adsorption model of two competitor species (for example diosgenin and stigmasterol). It has to be mentioned that the numerical form of a mathematical model, even if it is not too complex, allows the evaluation and the scale-up of the process. The considered values of a_{1A}, b_{1A}, k_{1A}, k_{2A}, Q_{LA}, a_{1B}, b_{1B}, k_{1B}, k_{2B}, Q_{LB} were obtained by using the experimental breakthrough curve and other experimental data [9] characterizing the adsorption equilibrium.

Table 1

Numerical formulation of the adsorption of two competitors in a fixed bed of MIPs

1	The known data are introduced as start data for the program (the bed height, the integration period, the flow rate through the MIP bed, the coefficient of axial diffusion, the kinetic parameter Q_L)
	$L := 40 \quad cm \qquad \tau := 6000\ s \qquad t_0 := 1000 \quad s \qquad d := 0.9 \cdot 10^{-2} \quad m$ $D_L := 1.4 \cdot 10^{-5}\ \frac{cm^2}{s} \qquad Q_L := 8 \cdot 10^{-5} \quad mol \cdot l^{-1}$
2	Are specified some of the kinetic parameters related to the sorption and desorption of species A and B
	$k_{1A} := 6 \cdot 10^{-2}\ s^{-1} \qquad k_{2A} := 1 \cdot 10^{-2}\ s^{-1} \qquad k_{1B} := 3 \cdot 10^{-2}\ s^{-1} \qquad k_{2B} := 2 \cdot 10^{-2}\ s^{-1}$
3	The kinetic specifications are supplemented.
	$a_1 := 5 \cdot 10^{-5} \quad a_2 := 100 \cdot 10^{-5} \quad a_3 := 1 \qquad a_4 := 1 \qquad a_5 := 1 \qquad a_6 := 10$
4	Are defined the parameters for the numerical integration.
	$N := 20 \qquad M := 1000 \qquad \Delta z := \frac{L}{N} \qquad \Delta t := \frac{\tau}{M}$
5	The numerical model is transpose with the univocity conditions including.

(C11 S11 C12 S12) = Controlled numerical solution of the process mathematically described through the set of equations (1)-(11)	
6	Are printed the matrices that give the composition of A component along the fixed bed, in solid and in liquid and the same for B component.
$C_{11}=$, $S_{11}=$, $C_{12}=$, $S_{12}=$	
7	Are identified the matrices, the breakthrough curves and the elution curves.

In order to describe the desorption of the components with this model, one can modify the *equations (2) and (3),* respectively *(8) and (9)*.

Next it is presented the power of the simulator in handling some case studies, each one having mentioned at the beginning the initial conditions. It will be tested the influence of the initial concentration in the adsorption case, the influence of the bed height and the influence of the flow rate. For all this case studies it will be presented the monocomponent adsorption and the competitive adsorption of two components.

4. Results

4.1. The influence of initial concentration, for adsorption case

The start data were: the height (length) of the bed (L), the integration period (τ), duration of experiment (t_0), the flow rate through the fixed bed (V), the coefficient of axial diffusion, (D_L), the kinetic parameter (Q_L) and the internal diameter (d = 0.9 cm).

$L := 60 \ \text{cm} \qquad \tau := 6000 \ \text{s} \qquad t_0 := 1000 \ \text{s}$

$D_L := 1.4 \cdot 10^{-5} \ \frac{\text{cm}^2}{\text{s}} \qquad Q_L := 8 \cdot 10^{-5} \ \text{mol} \cdot \text{l}^{-1}$

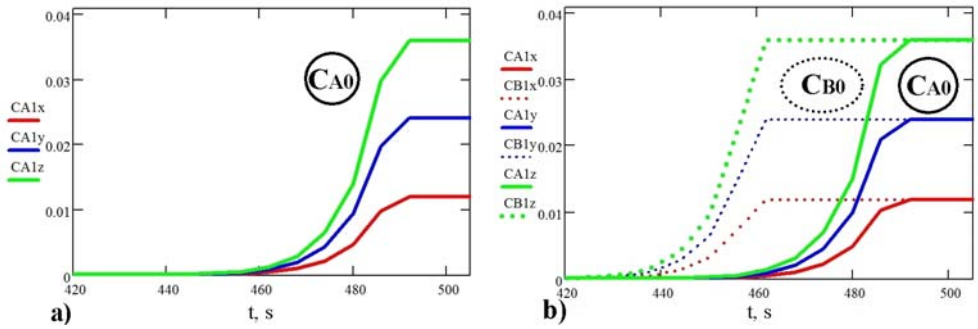

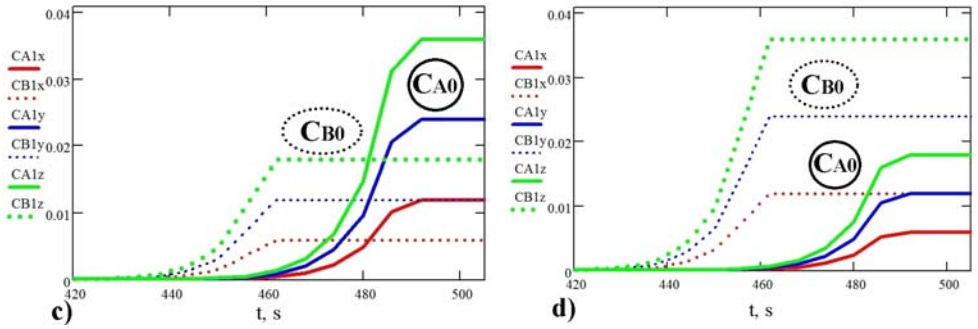

Fig. 2. The influence of the initial concentration: a) at monocomponent adsorption; b) at competitive adsorption with the template's concentration **equal** to competitor's one; c) at competitive adsorption with the template's concentration ***double*** than competitor's; d) at competitive adsorption with the competitor's concentration *double* than template's.

As initial concentrations, there will be used the values 0.012, 0.024 and 0.036 g/L for the monocomponent adsorption (C_{A0}) as well as for the competitive adsorption, where it will be considered three situations: 1) $C_{A0} = C_{B0}$ (*Fig. 2.b*); 2) $C_{A0} = 2 \cdot C_{B0}$ (*Fig. 2.c*); 3) $C_{A0} = 0.5 \cdot C_{B0}$ (*Fig. 2.d*). The flow rate for the presented case is $V_1 = 0.15$ cm·s^{-1} and the height of the MIP bed H = L = 60 cm.

From *Fig. 2.a)* it is noticed that with the increasing of the initial concentration, the breakthrough of the MIP bed starts sooner, as expected.

For a better understanding of the competitive adsorption inside the MIP particles using the simulator it is necessary the focusing on the parameters that define the adsorption and desorption processes, namely the rate constants for adsorption and desorption for each component.

$$k_{1A} := 6 \cdot 10^{-2}\ s^{-1} \qquad k_{2A} := 1 \cdot 10^{-2}\ s^{-1} \qquad k_{1B} := 3 \cdot 10^{-2}\ s^{-1} \qquad k_{2B} := 2 \cdot 10^{-2}\ s^{-1}$$

For component 1 (A), which is the template (diosgenin) used for imprinting the MIP-AN:AA-80:20 pearls, it was considered an adsorption rate constant (k_{1A}) two times higher than the one of the competitor (k_{1B}) in order to suggest a higher affinity of the MIP's binding sites for the template. For the desorption process it was considered a desorption rate constant two times smaller for the template ($k_{2A} = 0.01$ s^{-1}) than for the competitor ($k_{2B} = 0.02$ s^{-1}) in order to suggest the involvement of the hydrogen bonds in retaining the template. If the constants' ratios for each component are calculated ($K_A = k_{1A}/k_{2A}$ for the template and $K_B = k_{1B}/k_{2B}$ for the competitor), it can be see that K_A is four times higher than K_B, which is synonym with an affinity four times higher for the template against the competitor. In literature and in experimental studies, affinities higher than 4 are frequently encountered. Also, from the comparison between the competitor's constants (k_{1B}-for adsorption, k_{2B}-for desorption), it can be seen that the model takes into consideration the fact that the competitor itself can be adsorbed by the porous MIP matrix, but non-specifically, fact observed during the lab

experiments. For this particular case it was obtained the *Fig. 2.b)*. The first component (A) traced with continuous lines breaks through the MIP bed with a delay of around 25 s, the simulator suggesting in this way the affinity of the binding sites for the first component (the template).

The *Figs. 2.c) and 2.d)* show two aspects of the adsorption process, when the template's concentration is double compared with the competitor, respectively when the competitor's concentration is double reported to template.

4.2. The influence of the height of MIP pearls' bed

The specific start data of this simulation are: the initial concentration of component A (0.024 g/L), which it will be considered identical with the concentration of component B in the case of competitive adsorption. All the other parameters remain unchanged (V_1 = 0.15 cm·s^{-1}), only the height of the MIP bed being varied (20, 40, and 60 cm).

$L := 40 \ \text{cm} \qquad \tau := 6000 \ \text{s} \qquad t_0 := 1000 \ \text{s} \qquad d := 0.9 \cdot 10^{-2} \ \text{m}$

$D_L := 1.4 \cdot 10^{-5} \ \frac{\text{cm}^2}{\text{s}} \qquad Q_L := 8 \cdot 10^{-5} \ \text{mol} \cdot \text{l}^{-1}$

$k_{1A} := 6 \cdot 10^{-2} \ \text{s}^{-1} \qquad k_{2A} := 1 \cdot 10^{-2} \ \text{s}^{-1} \qquad k_{1B} := 3 \cdot 10^{-2} \ \text{s}^{-1} \qquad k_{2B} := 2 \cdot 10^{-2} \ \text{s}^{-1}$

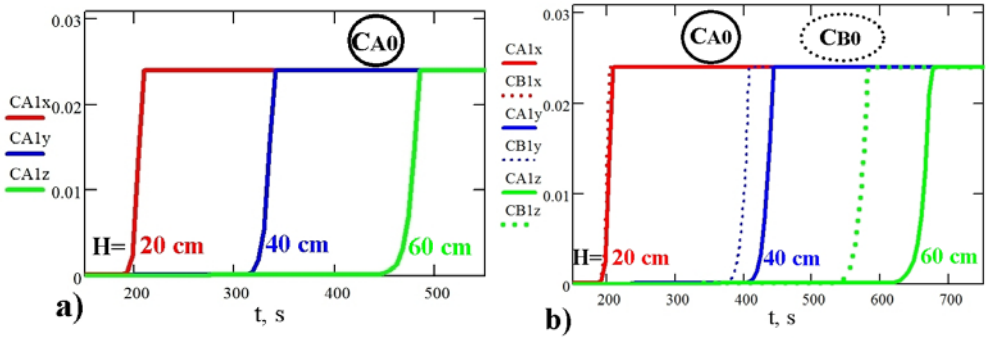

Fig. 3. The influence of the MIP bed height: a) at monocomponent adsorption; b) at competitive adsorption

The bed height has direct influence on the time at which the breakthrough starts. At a higher MIP bed (60 cm), the necessary time for breakthrough is longer (around 620 s), but, in the case of competitive adsorption, this is an advantage because it allows the good separation of components.

The influence of the bed height becomes important in the case of competitive adsorption between two components. In *Fig. 3.b)* it can be observed how it is improved the separation by increasing the height of the fixed bed, in this

way being increased the retention time of the selective component on the binding sites. For a fixed bed of 20 cm, the breakthrough starts after 200 s, but the separation of the components is not possible, both components eluting together. On the 40 cm fixed bed the separation is still possible, although slightly harder.

4.3. The influence of solvent flow rate

The start data for the study of the influence of the solvent flow are: the height of the MIP bed (40 cm) and the initial concentration of component A (0.024 g/L), identical with the initial concentration of component B. The other parameters remain unchanged, while the flow rate will take the values 0.15, 0.30, and 0.45 cm s^{-1}.

$L := 40 \ \text{cm}$ $\tau := 6000 \ \text{s}$ $t_0 := 1000 \ \text{s}$ $d := 0.9 \cdot 10^{-2} \ \text{m}$

$D_L := 1.4 \cdot 10^{-5} \ \frac{\text{cm}^2}{\text{s}}$ $Q_L := 8 \cdot 10^{-5} \ \text{mol} \cdot \text{l}^{-1}$

$k_{1A} := 6 \cdot 10^{-2} \ \text{s}^{-1}$ $k_{2A} := 1 \cdot 10^{-2} \ \text{s}^{-1}$ $k_{1B} := 3 \cdot 10^{-2} \ \text{s}^{-1}$ $k_{2B} := 2 \cdot 10^{-2} \ \text{s}^{-1}$

$V_1 := 0.15 \ \text{cm} \cdot \text{s}^{-1}$ $V_2 := 0.3 \ \text{cm} \cdot \text{s}^{-1}$ $V_3 := 0.45 \ \text{cm} \cdot \text{s}^{-1}$

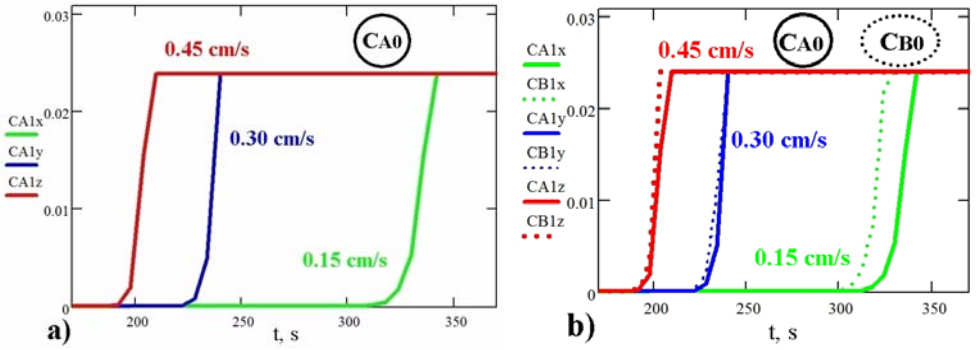

Fig. 4. The influence of the flow rate in the case of: a) non-competitive adsorption of diosgenin; b) competitive adsorption of diosgenin (A) against a competitor (B).

In *Fig. 4.a)* it is evidenced the effect of the flow rate through the MIP bed on the breakthrough dynamics of component A. As the model shows, the higher the flow rate is, the faster the breakthrough takes place.

The importance of the flow rate on the separation of two components becomes obvious in the *Fig. 4.b).* At high flow rates, both compounds elute together from the MIP bed, while operating the solution at smaller flow rates allows the separation of the components.

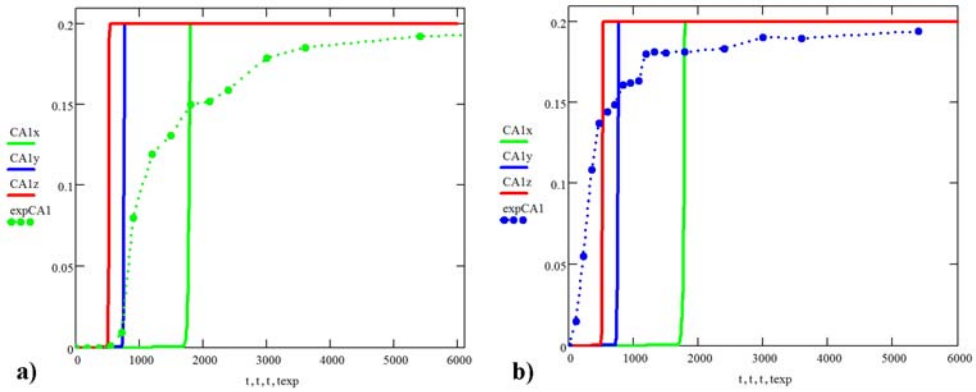

Fig. 5. Two experimental curves obtained in the following conditions: H = 44 cm, $D_L = 1.125 \cdot 10^{-5}$ cm^2/s, $V_{green} = 0.05$ cm/s, $V_{blue} = 0.1$ cm/s, $V_{red} = 0.15$ cm/s.

The experimental curves presented in *Fig. 5* suggest that the hypothesis of linear adsorption into MIP pearls (equation 5) is a significant approximation that requires improvement. Further studies will investigate other hypotheses regarding the type of adsorption in molecularly imprinted polymers, like adsorption after power law or hyperbolic law.

5. Conclusions

The mathematical model designed for the study of adsorption-desorption processes that take place in a fixed bed of selective polymer pearls obtained by molecular imprinting allowed the obtaining of breakthrough curves of one or two components in specific operating conditions. Three of the main operating parameters usually varied in the adsorption process on a fixed bed, meaning the initial concentration, the bed height, and the solvent flow rate, were studied with the help of the mathematical model. For the first parameter, the simulator evidenced that a higher concentration in the initial solution lead to a faster breakthrough of MIP pearls' bed. The model allows also the variation of the concentration ratio between components and predicts the possible evolution.

The influence of the second parameter, the height (length) of the MIP bed, can also be studied on the developed mathematical model. The simulator shows that this parameter has a great importance, having the property of inducing the separation of components from a mixed solution. A fixed bed of 20 cm can not perform the separation of two components in the studied conditions. If the fixed bed has a height of 40 cm, then the separation becomes possible, but a height of 60 cm has an increased performance. For the third parameter, the flow rate through the fixed bed, it was observed that a higher flow rate leads to a faster breakthrough in the case of monocomponent adsorption, but this is a disadvantage if the separation of components is needed. If a good separation is necessary, then a

lower flow rate, combined with a higher fixed bed height has to be taken into consideration. The developed mathematical model represents a good start for the study of various situations of mass transfer in MIP beds and in similar systems due to the fact that different hypotheses can be easily investigated and compared with experimental case studies. Further improvements of current mathematical model could transform it into a powerful scale-up instrument for selective separation processes.

Acknowledgements

This work has been funded by the Sectoral Operational Programme Human Resources Development 2007-2013 of the Ministry of European Funds through the Financial Agreement POSDRU/159/1.5/S/134398 and partially by the project BD81 from CNCSIS.

R E F E R E N C E S

[1] *Ş.O. Dima, C.A. Nicolae, T.V. Iordache, O. Chetraru, W. Meouche, V.A. Faraon, D. Donescu*, "Thermal analyses as tools for proving the molecular imprinting with diosgenin and sclareol in acrylic copolymer matrices", J. Therm. Anal. Calorim., **vol. 120**, no. 2, 2015, pp. 1107-1118.

[2] *H.Y. Zheng, M. Yoshikawa*, "Molecularly imprinted cellulose membranes for pervaporation separation of xylene isomers", J. Membr. Sci., **vol. 478**, 2015, pp. 148-154.

[3] *E. Benito-Peña, V. González-Vallejo, A. Rico-Yuste, L. Barbosa-Pereira, J. M. Cruz, A. Bilbao, C. Alvarez-Lorenzo, M. C. Moreno-Bondi*, "Molecularly imprinted hydrogels as functional active packaging materials", Food Chem., **vol. 190**, 2016, pp. 487-494.

[4] *M.J. Whitcombe, N. Kirsch, I.A. Nicholls*, "Molecular imprinting science and technology: a survey of the literature for the years 2004-2011", J. Mol. Recognit., **vol. 27**, no. 6, 2014, pp. 297-401.

[5] *J.K. Awino, Y. Zhao*, "Polymeric nanoparticle receptors as synthetic antibodies for nonsteroidal anti-inflammatory drugs (NSAIDs)", ACS Biomater. Sci. Eng., **vol. 1**, no. 6, 2015, pp. 425-430.

[6] *M. Bougrini, A. Florea, C. Cristea, R. Sandulescu, F. Vocanson, A. Errachid, B. Bouchikhi, N. El Bari, N. Jaffrezic-Renault*, "Development of a novel sensitive molecularly imprinted polymer sensor based on electropolymerization of a microporous-metal-organic framework for tetracycline detection in honey", Food Control, **vol. 59**, 2016, pp. 424-429.

[7] *Y.W. Tang, J.X. Lan, X. Gao, X.Y. Liu, D.F. Zhang, L.Q. Wei, Z.Y. Gao, J.R. Li*, "Determination of clenbuterol in pork and potable water samples by molecularly imprinted polymer through the use of covalent imprinting method", Food Chem., **vol. 190**, 2016, pp. 952-959.

[8] *Y. Nakai, M. Yoshikawa*, "Cellulose as a membrane material for optical resolution", Polym. J., **vol. 47**, 2015, pp. 334-339.

[9] *Ş.O. Dima, W. Meouche, T. Dobre, T.V. Iordache, A. Sarbu*, "Diosgenin-selective molecularly imprinted pearls prepared by wet phase inversion", React. Funct. Polym., **vol. 73**, no. 9, 2013, pp. 1188-1197.

[10] *M. Porcel-Valenzuela, A. Salinas-Castillo, E. Morallón, F. Montilla*, "Molecularly imprinted silica films prepared by electroassisted deposition for the selective detection of dopamine", Sens. Actuators B: Chem., **vol. 222**, 2016, pp. 63-70.

[11] *T.V. Nicolescu, A. Sarbu, M. Ghiurea, D. Donescu*, "Influence of crosslinker/porogen ratio upon imprinted polymer parameters", U.P.B. Sci. Bull., Series B, **vol. 73**, no. 1, 2011, pp. 163-172.
[12] *J.L. Morrison, M. Worsley, D.R. Shaw, G.W. Hodgson*, "The nature of the specificity of adsorption of alkyl orange dyes on silica gel", Canad. J. Chem. – Rev. Canad. Chim., **vol. 37**, 1959, pp. 1986-1995.
[13] *X. Zhang, M.Y. Zhu, S. J. Li*, "<Key-vs.-Lock>-like polymer reactor made of molecularly imprinted polymer containing metal nanoparticles", J. Inorg. Org. Polym. Mater., **vol. 24**, no. 5, 2014, pp. 890-897.
[14] *Ş.O. Dima, T. Dobre, A. Sarbu, M. Ghiurea, C. Bradu*, Proofs for molecular imprinting of an acrylic copolymer by phase inversion, U.P.B. Sci. Bull., Series B, **vol. 71**, no. 4, 2009, pp. 21-30.
[15] *D.L. Huang, R.Z. Wang, Y.G. Liu, G.M. Zeng, C. Lai, P. Xu, B.A. Lu, J.J. Xu, C. Wang, C. Huang*, "Application of molecularly imprinted polymers in wastewater treatment: a review", Environ. Sci. Pollut. Res., **vol. 22**, no. 2, 2015, pp. 963-977.
[16] *S. Antic, L. Djordjevic, K. Kostic, A. Lisec*, "Dynamic discrete simulation model of an inventory control with or without allowed shortage", U.P.B. Sci. Bull., Series A, **vol. 77**, no. 1, 2015, pp. 163-176.
[17] *B. Sandu (Ohreac), T. Dobre, O.C. Pârvulescu*, "Modelling and optimization of acetone-butanol-ethanol fed-batch biosynthesis", U.P.B. Sci. Bull., Ser. B, **vol. 76**, no. 4, 2014, pp. 45-58.
[18] *G. Nechifor, D.E. Pascu, M. Pascu (Neagu), G.A. Traistaru, P.C. Albu*, "Comparative study of Temkin and Flory-Huggins isotherms for adsorption of phosphate anion on membranes", U.P.B. Sci. Bull., Series B, **vol. 77**, no. 2, 2015, pp. 63-72.
[19] *R. Aris*, "Interpretation of sorption and diffusion data in poros solids", Ind. Eng. Fundam., **vol. 22**, 1983, pp. 150-154.
[20] *D. Do, R.G. Rice*, "On the relative importance of pore and surface diffusion in non-equilibrum adsorption rate processes", Chem. Eng. Sci. **vol. 42**, 1987, pp. 2269-2284.
[21] *A.K. Bordbar, A. A. Saboury, A. A. Moosavi*, "The shapes of Scatchard plots for systems with two sets of binding sites", Biochem. Educ., **vol. 24**, 1996, pp. 172-175.
[22] *J.A. García-Calzon, M.E. Diaz-Garcia*, "Characterization of binding sites in molecularly imprinted polymers", Sens. Actuators, B, **vol. 123**, 2007, pp. 1180–1194.
[23] *Ş.O. Dima*, "Equilibrium and kinetic isotherms and parameters for molecularly imprinted with sclareol poly(acrylonitrile-co-acrylic acid) matrix", Polym. Eng. Sci., **vol. 55**, no. 5, 2015, pp. 1152-1162.
[24] *M. Yoshikawa, J. Izumi, T. Kitao, S. Koya, S. Sakamoto*, "Membranes for enantioselective separation: Synthesis and characterization", Preprints 16th Ann. Meet. Membr. Soc. Japan, 1994, A1-1-1.
[25] *M. Yoshikawa, J. Izumi, T. Kitao, S. Koya, S. Sakamoto*, "Molecularly imprinted polymeric membranes for optical resolution", J. Membr. Sci., **vol. 108**, 1995, 171-175.
[26] *M. Yoshikawa, J. Izumi, T. Kitao, S. Sakamoto*, "Alternative molecularly imprinted polymeric membranes from a tetrapeptide residue consisting of D- or L-amino acids", Macromol. Rapid Commun., **vol. 18**, 1997, pp. 761-767.
[27] *O. Smigelschi, A. Woinaroschi,* Process Optimzation, Ed. Tehnica, Bucharest, 1980.
[28] *T. Dobre, J.M. Sanchez*, Chemical Engineering-Modelling, Simulation and Similitude, Wiley VCH, 2007.